applied sciences

MDPI

Article

Reliability of Field Experiments, Analytical Methods and Pedestrian's Perception Scales for the Vibration Serviceability Assessment of an In-Service Glass Walkway

Chiara Bedon * and Marco Fasan

Department of Engineering and Architecture, University of Trieste, 34127 Trieste, Italy; mfasan@units.it
* Correspondence: chiara.bedon@dia.units.it; Tel.: +39-040-558-3837

Received: 8 April 2019; Accepted: 7 May 2019; Published: 11 May 2019

Abstract: The vibration performance of pedestrian structures attracts the attention of several studies, especially with respect to unfavorable operational conditions or possible damage scenarios. Given a pedestrian system, specific vibration comfort levels must be satisfied in addition to basic safety requirements, depending on the class of use, the structural typology and the materials. To this aim, guideline documents of the literature offer simplified single-degree-of-freedom (SDOF) approaches to estimate the maximum expected vibrations and to verify the required comfort limits. Most of these documents, however, are specifically calibrated for specific scenarios/structural typologies. Dedicated methods of design and analysis, in this regard, may be required for structural glass pedestrian systems, due to their intrinsic features (small thickness-to-size ratios, high flexibility, type and number of supports, live-to-dead load ratios, use of materials that are susceptible to mechanical degradation with time/temperature/humidity, etc.). Careful consideration could be then needed not only at the design stage, but also during the service life of a given glass walkway. In this paper, the dynamic performance of an in-service glass walkway is taken into account and explored via field vibration experiments. A set of walking configurations of technical interest is considered, involving 20 volunteers and several movement features. The vibration comfort of the structure is then assessed based on experimental estimates and existing guideline documents. The intrinsic uncertainties and limits of simplified approaches of literature are discussed, with respect to the performance of the examined glass walkway. In conclusion, the test predictions are also used to derive "perception index" data and scales that could support a reliable vibration comfort assessment of in-service pedestrian glass structures.

Keywords: vibration serviceability; laminated glass; glass walkway; field vibration experiments; dynamic properties; human-structure interaction (HSI), human comfort; perception scales

1. Introduction

Load-bearing structural glass elements in buildings can take the form of simple members (columns, beams and plates) but also complex assemblies. While the research community is spending efforts for the development/refinement of safe and optimized rules for the design of glass structures (see for example [1–3], etc.), most of the current issues are related to their intrinsic vulnerability.

This is also the case of glass structures under dynamic/impact loads, or complex systems and glass stairs ([4–14], etc.) where—in addition to conventional safety design requirements ([1,2] and Section 2)—excessive vibrations may involve unfavorable feelings and require dedicated interventions, at the design stage as well as during the service life. The dynamic performance of a given glass structure can be in fact affected by several parameters, like the loading features, the structural geometry,

the properties of the involved materials and bonding layers or the presence of mechanical and adhesive restraints that could manifest a time/temperature/humidity-varying flexibility (see Figure 1 and [15,16]). Even more attention is required for pedestrian glass structures that could be subjected to severe operational conditions, with pronounced human structure interaction (HSI) phenomena [17,18].

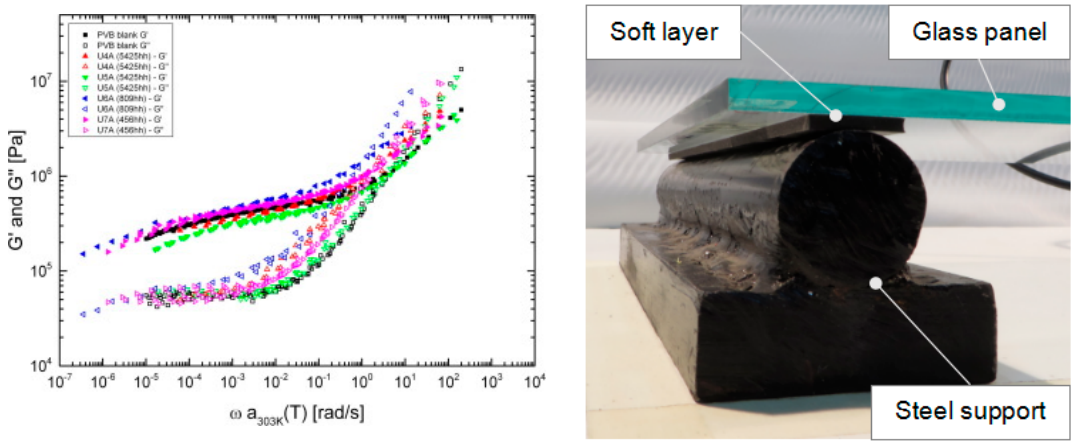

(**a**) (**b**)

Figure 1. Dynamic performance of glass members: (**a**) Sensitivity of polyvinyl butyral (PVB®) stiffness to humidity/loading frequency (reproduced from [15] with permission from Elsevier, license n. 4585281507083, May 2019) and (**b**) flexible restraints (reproduced from [16] under CC BY 4.0 license).

This paper focuses on the vibration serviceability assessment of an in-service glass walkway in Italy. The pedestrian structure (see Figure 2 and Section 3) was built in the early 2000, in the monumental building of the Basilica of Aquileia (UNESCO World Heritage Site). The original design of the indoor suspension system resulted in a sandwich laminated glass (LG) slab, composed of a triple fully tempered (FT) section and polyvinyl butyral (PVB®) bonding layers. A sacrificial annealed (AN) layer was placed on the top of each LG panel, to obtain an LG + AN resisting section. A series of steel tendons and frame members were then used to support the glass plates, for up to ≈140 square meters of transparent walking surface.

(**a**) (**b**)

Figure 2. In-service pedestrian system object of analysis: (**a**) General/front view (photo by C. Bedon, courtesy of So.Co.Ba) and (**b**) nominal cross-section of the glass slab.

The research outcomes presented in this paper follow and extend the preliminary experimental investigation summarized in [16], where the vibration performance of monolithic glass samples under soft impact was assessed as a function of flexible mechanical supports (Figure 1b), including analytical calculations derived from classical dynamic theories [17] and Finite Element (FE) parametric studies (ABAQUS [19]). In addition, the current investigation aims at further exploring the vibration response of the glass walkway discussed in [20] for diagnostic purposes. More in detail, the attention is

spent for the analysis of the vibration comfort levels that the system can actually offer, under several loading scenarios of technical interest. To this aim, original field experiments inclusive of 26 setup configurations and 20 volunteers are first presented. The sensitivity of fundamental dynamic estimates is hence explored, based on the experimental outcomes, with respect to several key parameters (i.e., walking features, number of occupants, ambient conditions, etc., see Section 4). Selected guideline documents for the human comfort assessment of pedestrian structures are then and applied to the case-study walkway, namely the Eurocode 0—Annex A2 [21] and ISO 10137 [22] methods, the SÉTRA approach [23] and the AISC Design Guide 11 [24], see Section 5. Finally, possible "perception index" and comfort scale evaluations are proposed in Section 6. As shown, their intrinsic advantage and potential – compared to existing analytical methods – is that the comfort level can be assessed as a function of multiple parameters of primary interest, like the walking features, or the imposed acceleration peaks, but also the feelings of the involved volunteers and their sensitivity to transparency (Figure 3).

Figure 3. The role of transparency on magnified human perception of vibrations and discomfort feelings for the glass walkway object of investigation (photo by C. Bedon, courtesy of So.Co.Ba).

2. Glass Structures and Vibrations

2.1. Safety Design Requirements for Glass Pedestrian Systems

Glass pedestrian systems are conventionally designed to satisfy a series of performance requirements under ordinary loads, namely related to the limitation of maximum deformations (service limit state—SLS) and tensile stresses (ultimate limit state—ULS), see [1–3]. Another key step of the design procedure is represented by the verification of the post-cracked residual resistance, stiffness and redundancy that glass systems (in case of possible damage) should be able to ensure at the collapse limit state (CLS). The optimal combination of glass type, number of glass layers (i.e., minimum three for pedestrian systems), thickness of glass and type/features of boundaries (with four side linear supports to privilege) generally allows designers to guarantee safe structural performances [1–3]. Besides the assessment of the conventional SLS, ULS and CLS requirements, however, special care should be spent for vibrations.

2.2. Vibration Analysis and Human-Structure Interaction (HSI) Phenomena

The vibration response of glass structures is a relatively recent research topic. Most of the literature studies include experimental, analytical and numerical analyses voted to explore the dynamic behavior

of single monolithic or LG members, with limited efforts for the performance assessment of complex assemblies, see for example [25–30].

As a general rule, glass slabs should be verified against vibrations under operational conditions in the same way of pedestrian structures composed of other constructional materials. Possible critical aspects of glass pedestrian structures, in this regard, can be represented by typically small thickness-to-size ratios, high flexibility and slenderness, unconventional or limited number/size of restraints (i.e., point supports, etc.). Additional uncertainties can then derive from the possible/progressive degradation of materials and restraints (i.e., Figure 1), hence resulting in even marked variations of the fundamental dynamic properties. Finally, HSI effects may be crucial [18,31–34]. From a mathematical point of view, a single stationary human body represents in fact a dynamic system able to interact with a given structure (see for example Figure 4a). Especially in presence of moving occupants or crowds (Figure 4b), HSI phenomena can hence involve complex effects, due to the occurrence of reciprocal motion forces and to the capacity of the occupants to change the dynamic features of a structure, over which they are [18]. Key parameters are represented by the motion features (i.e., pacing frequency and phase, walking speed, stride length, etc.), and dedicated tools are necessarily required for reliable analyses. A given pedestrian structure must in fact satisfy the general equation of motion:

$$M\ddot{x}(t) + C(t) + Kx(t) = P(t) \tag{1}$$

with M, C and K denoting the modal mass, damping and stiffness matrices, $P(t)$ the imposed external (periodic) force reproducing the motion of occupants and $x(t)$ the vertical displacement vector.

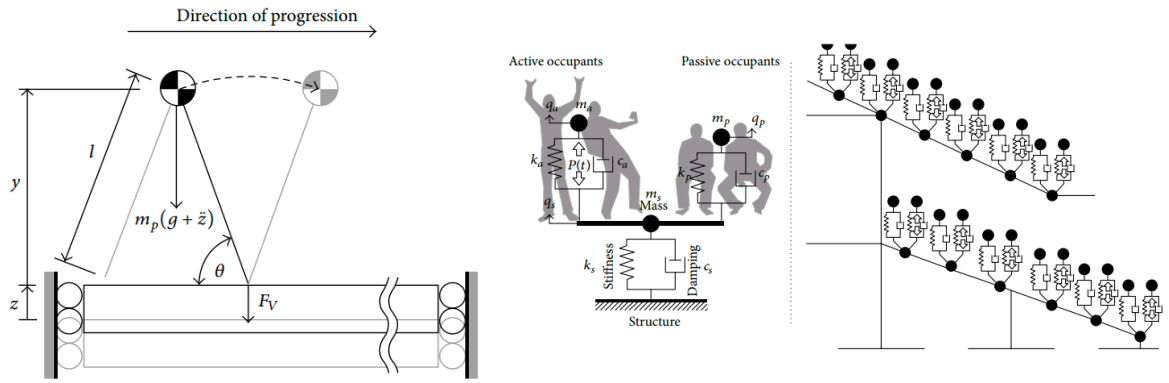

(**a**) (**b**)

Figure 4. Mathematical models for human-structure interaction (HSI) calculations of pedestrian structures: (**a**) Inverted pendulum approach and (**b**) crowd effects on stadium structures. Figures reproduced from [18] under CC BY 4.0 license.

As far as the pedestrian systems of Figure 3 are occupied ("os"), it is expected that the fundamental frequency and the corresponding modal damping modify, with respect to the empty structure ("es"), that is:

$$f_{os} = \frac{1}{2\pi} \cdot \sqrt{\frac{k_{os}}{m_{os}}} \neq f_{es} \tag{2}$$

and

$$\xi_{os} = \frac{c_{os}}{2\sqrt{k_{os} m_{os}}} \neq \xi_{es} \tag{3}$$

Several literature contributions demonstrated that [18]:

- standing people commonly reduces the frequency of an occupied system, that is $f_{os} < f_{es}$, while;
- walking occupants generally manifest in a frequency increase, $f_{os} > f_{es}$.

Moreover:

- when the natural frequency of walking bodies (f_p) is less than the frequency of the empty structure (f_{es}), it is expected that $f_{os} > f_{es}$;
- when $f_p > f_{es}$, otherwise, it is typically observed that $f_{os} < f_{es}$;
- the effects of walking human bodies are more pronounced as the number of pedestrian increases;
- and finally, damping is always expected to increase for an occupied system, i.e., $\xi_{os} > \xi_{es}$.

The common assumption of the general considerations listed above is that they are strictly related to a series of multiple aspects, including the mechanical features of the structure under analysis and the role that human bodies can induce in the vibration response of the empty system. Accordingly, refined design approaches are required for the assessment of comfort levels (see for example [35–37], etc.). Even more advanced calculation strategies can be required for pedestrian systems in which the position and movement of the occupants can be relevant [38–42]. Starting from these conditions, the uncertainty of glass structures is that LG composite sections require careful estimates of the actual bending properties and/or restraints (see also [16,20]). Most of the HSI investigations of literature, in addition, have been carried out on various typologies of footbridges and floors made of timber, precast reinforced concrete, steel or hybrid members (see [43–46], etc.). Otherwise, studies focused on the vibration performance of glass pedestrian structures are still limited.

3. Description of the Glass Walkway Object of Analysis

3.1. Geometry and Materials

The in-service walkway was designed to protect the early Christian floor mosaics of the central nave of the Basilica (≈750 square meters), minimizing the impact of the structure on the monument. In accordance with Figure 2a, the system actually includes 79 LG + AN panels and can be roughly described in the form of a global T-shape, with a main entrance platform (allowing the communication between the central nave (on the right side) and the adjacent crypt (on the left)), and a further pedestrian path, crossing longitudinally the central nave of the church.

The main entrance platform consists in a simply supported slab, with a global beam-like bending behavior ensured by four longitudinal steel-glass girders (14.5 m their span), see Figure 5.

Special care is spent in this paper for the central nave path, see Figure 6, consisting of a series of independent LG + AN panels, with two-side linear supports along the short edges and variable span (comprised between 2.5 m and 2.65 m, depending on the actual distance of the columns). Three adjacent panels are used in the width of the path (Figure 6a). Among them, the central panel is considered, being characterized by a maximum width of 1.65 m, and by the presence of three steel tendon pairs (10 mm the diameter, with 0.75 m their distance) that are intended to act as mid-span unilateral supports for the glass slab (see for example the T1-to-T3 tendons in Figure 6a, or the lateral view of Figure 6c).

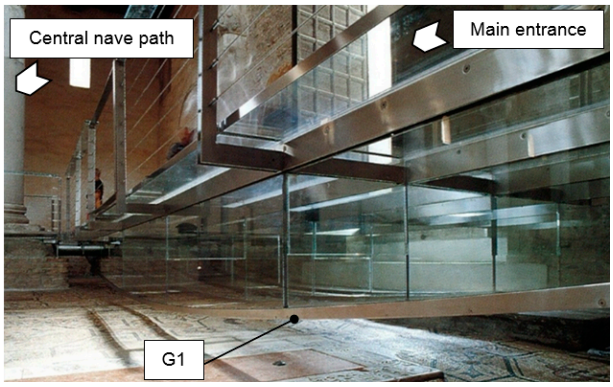

(**a**)

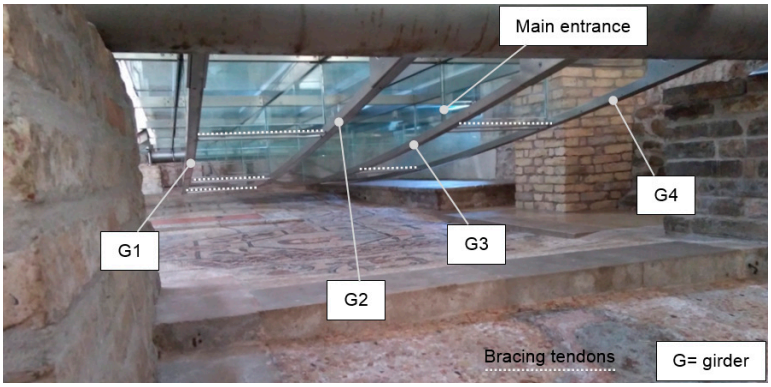

(**b**)

Figure 5. Main entrance suspension platform: (**a**) Front/bottom view and (**b**) detail bottom view, with evidence of longitudinal girders and tendons (photos by C. Bedon, courtesy of So.Co.Ba).

3.2. *Vibration Issues and Previous Research on the Empty Glass Walkway*

The selected LG + AN panel of Figure 6 was realized in the form of a sandwich thickness with 42 mm of glass (see also the detail of Figure 2b), with 4.37 square meters of pedestrian surface and a total glass mass M_{glass} = 460 kg. The primary goal of the original design was to ensure the slab—based on a global beam-like bending behavior—appropriate structural performances under live loads.

It was shown in [20], however, that the empty system is actually characterized by a mean experimental frequency f_{es} = 15.1 Hz (with ξ_{es} = 1.15% the corresponding damping). Such a value is relatively low, compared to the "design" configuration (with f_{es} = 19.5 Hz, that is ≈−30%), and the marked frequency decrease was found to mainly derive from the stiffness degradation of the bonding PVB foils (due to long term phenomena and unfavorable ambient conditions), with respect to their nominal mechanical properties (with G_{int} ≈ 1.35 MPa the shear stiffness of PVB from vibration experiments). Compared to [20], careful consideration is hence spent in this paper for the experimental analysis of the occupied system in service conditions, giving evidence of its dynamic behavior under various scenarios of technical interest.

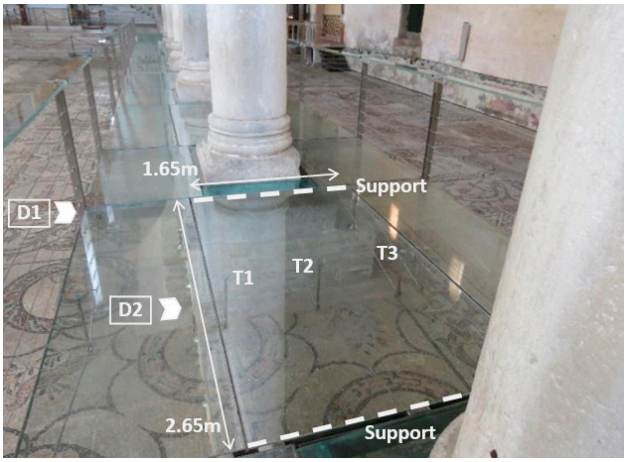

(**a**)

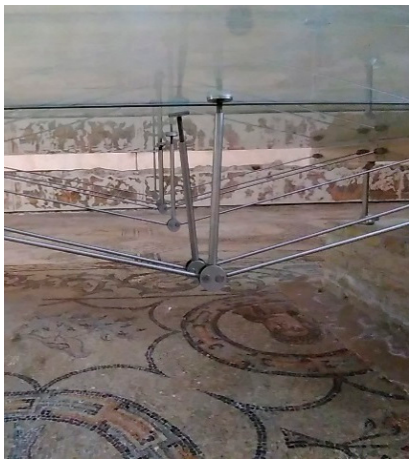

(**b**) (**c**)

Figure 6. Reference two-side supported panel along the central nave path: (**a**) General view, with (**b**–**c**) D1 and D2 details (reproduced from [20] with permission from Elsevier, license n. 4585290441718, May 2019).

4. Experimental Analysis of the Occupied Walkway

Dynamic field tests were performed under pedestrian excitation, for the two-side supported panel of Figure 5. The experimental measurements were collected in two different periods of the year, with variations in the reference temperature and humidity (see Table 1). In doing so, the test instruments and methods were kept identical.

Table 1. Reference configurations for the field vibration tests.

Period	Month	Test Time	Temperature (°C)		Relative Humidity (%)
			Daily (Max-Min)	Test (Mean)	(Test Time)
P#1	March 2019	9–10 a.m.	7.5/15.0	13.2	76
P#2	November 2017	8–10 a.m.	4.1/7.2	6.5	87

The acceleration measurements were performed using six micro electro-mechanical system (MEMS) triaxial accelerometers prototyped in [47]. Their position was aimed at properly capturing the fundamental mode of the system, based also on past studies (see [20] and Figure 7).

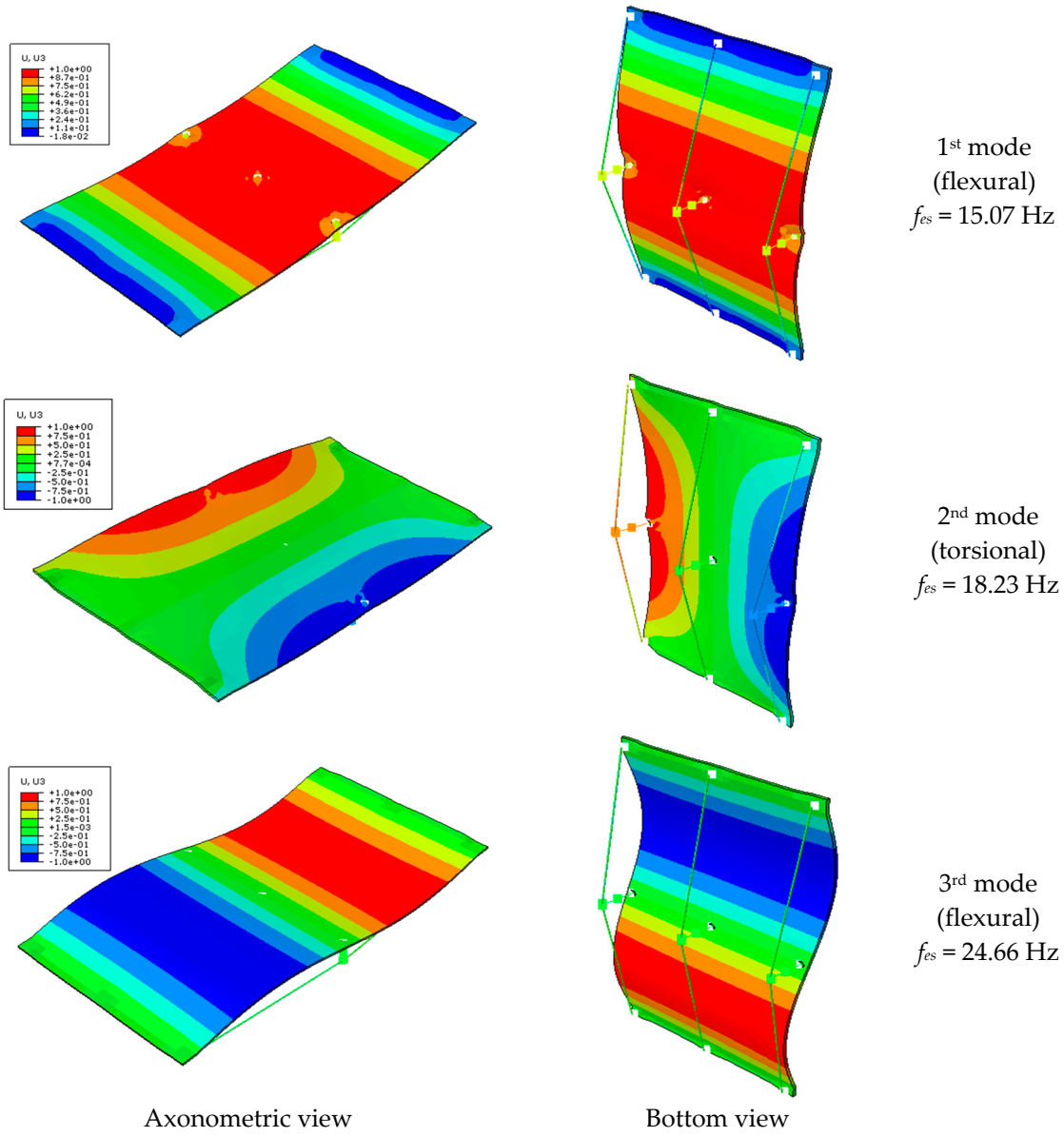

Figure 7. First vibration modes and frequencies of the empty structure (ABAQUS, axonometric and bottom view). Numerical study derived from the FE model presented in [20].

The imposed random vibrations involved up to 20 adults (with ≈80 kg their average weight). Most of the walking conditions were detected to reproduce realistic operational conditions for the structure, i.e., with visitors moving slowly by small groups, standing on the walkway, etc. In Table 2, the overall setup features are grouped by period of the year (P#*n*, see Table 1), and listed by total number of occupants (p). A further distinction is provided in terms of occupation density d (p/walking area), number of standing/walking persons and qualitative features of movements.

The tests were carried out with the support of a variable number of male and female volunteers, asked to walk back and forth (or randomly) on the monitored system. The step frequency of normal or consistent walks was established in the conventional range of 1.5–2.5 Hz. In some cases, additional measurements were carried out with a single occupant standing on the structure, by imposing an impulsive vibration (in-place jump). Special care was hence spent for the analysis of major dynamic effects due to (a) unsynchronized motion of the occupants ($p \geq 2$), (b) normal or consistent walk of the occupants, (c) regular (i.e., longitudinally to the central nave, back and worth) or irregular (i.e., random) walking path.

Table 2. Examined test scenarios for the system object of analysis (Figure 6).

Test Scenario	Occupants		Standing			Walking			Period
	Total p	Density p/m^2	Number	Position	Notes	Number	Position	Notes	
CN#1	1	0.228	-	-	-	1	Center	Jump	P#1
CN#2	1	0.228	-	-	-	1	Center	Jump	P#1
CN#3	1	0.228	-	-	-	1	Center	Jump	P#1
CN#4	1	0.228	-	-	-	1	Center	Jump	P#1
CN#5	2	0.457	1	Center	-	1	Overall	Normal Random	P#1
CN#6	3	0.686	1	Center	-	2	Overall	Normal Random	P#1
CN#7	3	0.686	1	Center	-	2	Overall	Normal Random	P#1
CN#8	4	0.914	1	Center	-	3	Overall	Normal Random	P#1
CN#9	4	0.914	3	Center	-	1	Overall	Normal Random	P#1
CN#10	6	1.372	3	Center	-	3	Overall	Normal Random	P#1
CN#11	6	1.372	3	Center	-	3	Overall	Normal Random	P#1
CN#12 CN#13	0	-	-	-	-	-	-	-	P#2
CN#14 to CN#19	1	0.228	-	-	-	1	Overall	Normal Random	P#2
CN#20 to CN#26	2	0.457	-	-	-	2	Overall	Normal Random	P#2

Legend (top view)

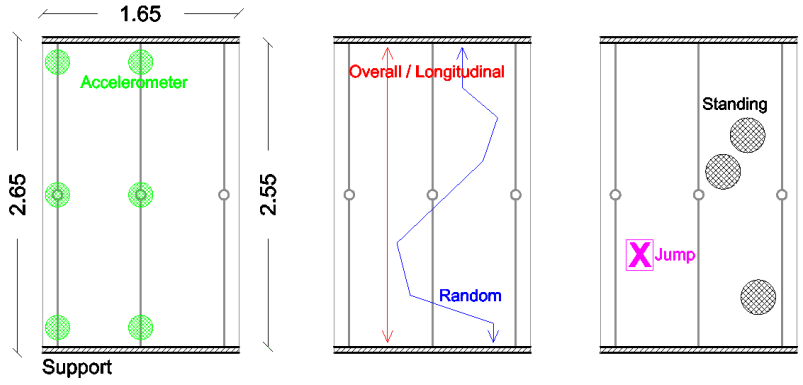

Dimensions in meters

5. Discussion of Test Results

5.1. Post-Processed Data

The acceleration data were recorded with a sampling frequency of 128 Hz, over a typical duration of 2 min. An example of accelerations and power spectral density functions is proposed in Figure 8, for the vertical and transverse directions. All the collected records were post-processed via the SMIT Toolsuite [48], based on the ERA-OKID-OO approach [49,50].

In doing so, the vertical accelerations were specifically investigated, being of primary interest for the examined system, with respect to mostly negligible longitudinal/transverse dynamic effects (i.e., Figure 8c,d).

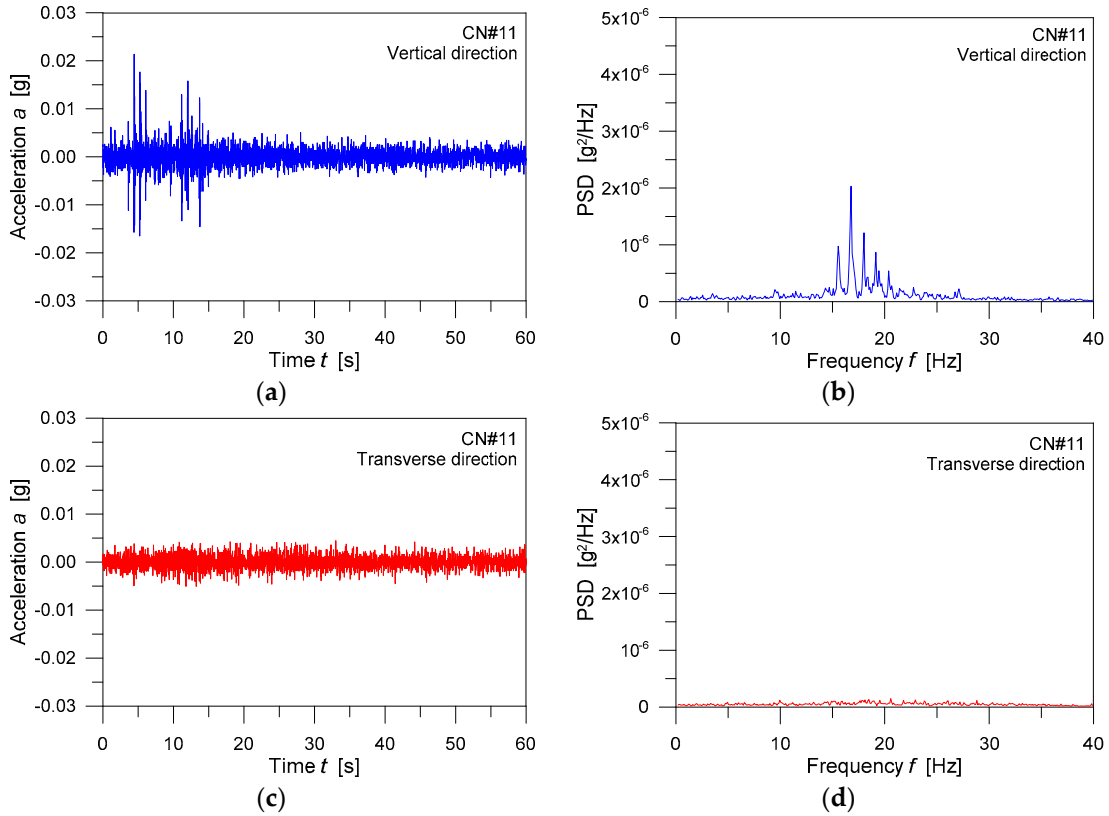

Figure 8. Examples of vibration measurements. (**a**,**c**) Acceleration-time history and (**b**,**d**) power spectral density functions under random walking traffic.

5.2. Dynamic Performance Parameters

The fundamental frequency f_{os} and damping ξ_{os} were estimated for all the test scenarios of Table 2. For each test configuration, the average estimate was then separately collected, based on the available instruments and records. Globally, rather stable predictions were obtained for a given CN#*n* scenario, with standard deviations less than ±0.06 Hz for frequency and ±0.08% for damping. The mean CN#12 and CN#13 estimates ($p = 0$), in addition, were taken into account as a reference configuration.

According to Figure 9a,c, it is possible to notice that as far as the full set of measurements is considered for the LG + AN panel in bending, a general increase with p is generally observed for the fundamental frequency $f_{os} > f_{es}$ and modal damping $\xi_{os} > \xi_{es}$. In Figure 9b, frequency scatter values are also proposed as a function of p, where:

$$\Delta_f = 100 \cdot \frac{(f_{os} - f_{es})}{f_{es}} \tag{4}$$

For reliable investigations, however, the variation of the dynamic parameters with p can offer only limited information, and multiple features should be necessarily taken into account (i.e., total mass M_p of the occupants, movement type, etc.). Ambient conditions (and their effects on the response of the PVB layers) represent another key aspect for the examined structure. Based on Table 1, for example, major effects were expected at the time of measurements for P#1 estimates, due to a potential decrease of the PVB stiffness resulting from:

- an increase of P#1 mean temperature (13.2 °C, in place of 6.5° of P#2 records);
- a longer life-time of the system (one year apart), with increased ageing phenomena (for the PVB foils but also for the other load-bearing components).

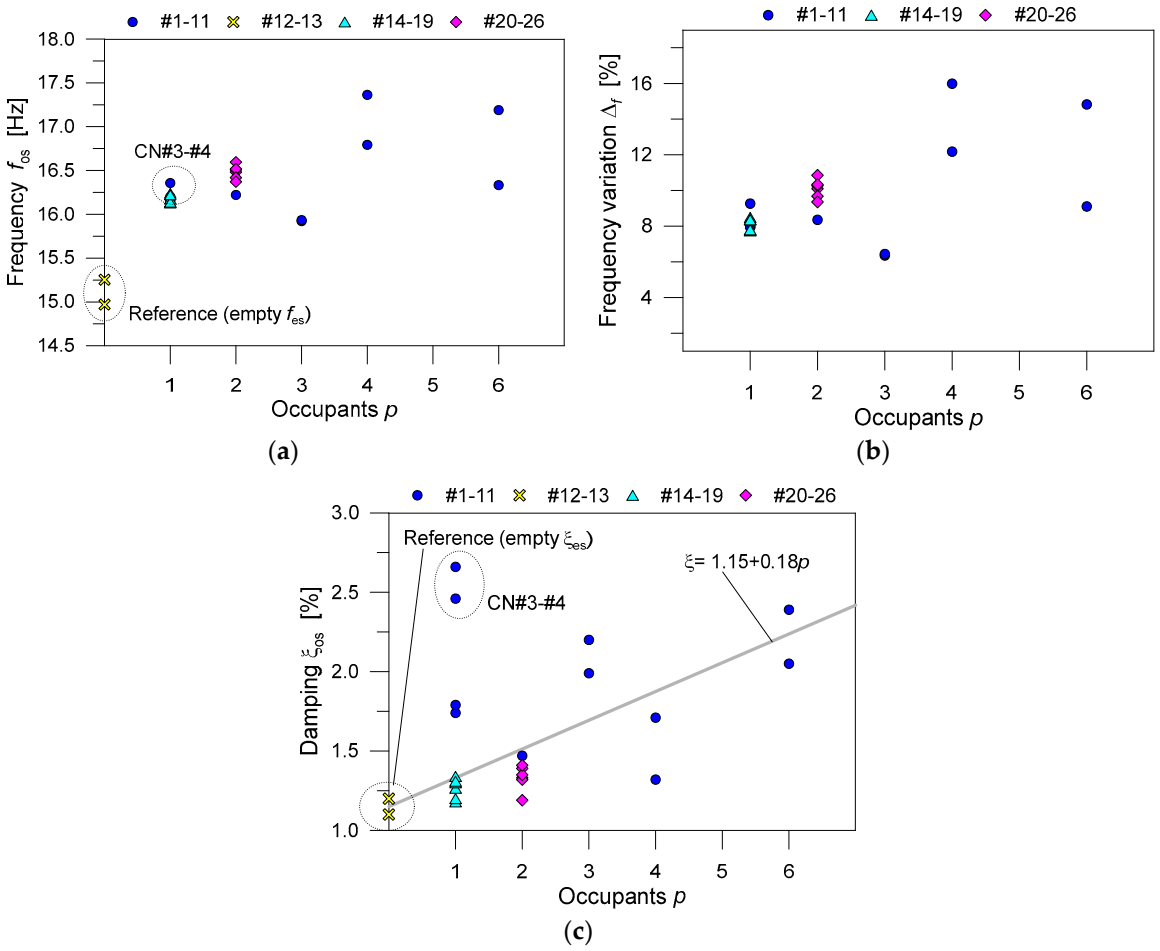

Figure 9. Variation of (**a**) frequency, (**b**) frequency scatter and (**c**) damping for the occupied system (average values).

A maximum scatter in the order of Δ_f = +15% was obtained (p = 4 and p = 6), compared to the empty structure. When p > 0, moreover, it can be perceived from Figure 9b that the f_{os} predictions are minimally affected by the ambient conditions herein investigated. For p = 1, even in the presence of a relatively wide range of imposed accelerations, Δ_f resulted in fact equal to +8.08% (P#1) and +8.34% (P#2) respectively, giving evidence of mostly negligible time/temperature/humidity effects, for the explored scenarios. This is in line also with the numerical findings reported in [20] for the empty structure, where it was shown that the vibration frequency can be highly sensitive to the stiffness of PVB foils (and hence to the global bending stiffness of the LG + AN section), but also other relevant aspects should be taken into account, like the loss of prestress in the bracing tendons, etc. The higher the ambient temperature (i.e., P#1 > P#2) and the lower the bending stiffness of the system, hence the lower the expected frequency f_{os} and the corresponding Δ_f.

According to Figure 9b, the added value of the experimental study reported herein is the role of time and humidity. More pronounced ageing phenomena (P#1 > P#2) and high temperature effects (P#1 > P#2) were observed to prevail on ambient humidity (P#2 > P#1). For p > 1 (P#1 scenarios), a mean frequency increase up to Δ_f = +15% was calculated. Given the same ambient conditions, such a result can be hence mostly justified by the combined number of standing/walking volunteers. This effect is also emphasized in Table 3, where the mean experimental Δ_f estimates (i.e., average results grouped by p) are not linearly proportional to p. Based on the dimensions of the panel (1.65 × 2.65 m^2), in this context, it can be reasonably expected a frequency increase up to Δ_f = +15%–20% for the

occupied structure (under similar ambient conditions). As far as the "added mass ratio" R_M is also taken into account, with:

$$R_M = \frac{M_p}{M_{glass}} \quad (5)$$

in Table 3 it can be also noticed that live loads are generally relevant, hence a further increase of dynamic effects and human perceptions can be expected (see Section 5.3).

Table 3. Average frequency variation and damping for the system (P#1).

Occupants p			Loading Condition (Mean)		Frequency Variation Δ_f (%)	Damping ξ (%)
Total	**Standing**	**Walking**	R_M **(Equation (5))**	a_{peak} **(%g)**		
1	0	1	0.182	7.13	+8.34	2.163
2	1	1	0.332	0.87	+8.35	1.470
3	2	1	0.546	0.91	+6.39	2.095
4	1	3	0.964	3.30	+14.08	1.515
6	3	3	1.350	3.27	+11.96	2.220

In terms of damping, see Figure 9c and Table 3, the presence of standing/walking people increased up to two times the capacity of the empty structure (ξ_{es} = 1.15%). The presented damping estimates, however, include several movement features, and also in-place jumps characterized by impulsive accelerations. As far as more detailed calculations are not available, a simple (ξ_{os}, p) linear correlation could be taken into account for preliminary estimates and in-service monitoring considerations on the two-side supported system, see Figure 9c.

5.3. Human Comfort and Vibration Serviceability Assessment Based on Existing Technical Documents

The acceleration records summarized in Section 5.2 were further assessed, with respect to conventional serviceability approaches in use for the comfort assessment of pedestrian structures [21–24]. According to the literature, the human body is mostly sensitive to frequencies in the range of 4 Hz to 8 Hz (i.e., typical range of most of the constructed floors), because it is associated to resonance phenomena with internal organs [18]. For this reason, several existing guideline documents for the comfort verification of human induced vibrations are based on a double evaluation check. The first one is related to the fundamental frequency of the system object of analysis (see for example [51]). For pedestrian systems with frequency in potential risk of resonance, detailed vibration analyses are commonly required, and these can take the form of refined Finite Element models or simple SDOF calculations. In both the cases, the goal is to evaluate the expected acceleration peaks (in the vertical and transverse directions), and compare them with threshold values that implicitly account for the comfort satisfaction of the occupants [37]. The potential of the technical documents recalled in this paper, see [21–24], is to offer practical methodologies for pedestrian systems, based on design charts or SDOF calculation approaches for equivalent, single occupant scenarios. However, according to the literature ([51–55], etc.), the possible limitations of these methods still require investigations. The reliability and accuracy of existing approaches, in particular, is a major problem for footbridges with high live-to-dead load ratios like the examined system (Table 3).

5.3.1. Eurocode 0—Annex A2 and ISO Criteria

The pedestrian comfort criterion of footbridges is conventionally defined by the Eurocode 0 (EC0)—Annex A2 in terms of an acceptable acceleration for any part of a given deck [21]. Annex A2 is specifically intended for bridges, while dedicated threshold accelerations (given as a function of the

vertical frequency f_v) are recommended for pedestrian structures. Generally, the acceleration peak must be limited to (values in m/s^2):

$$a_{max} = min\begin{cases} 0.5\sqrt{f_v} \\ 0.7 \end{cases} \quad (6)$$

When the deck frequency exceeds 5 Hz, in addition, it may be assumed that no further verifications are required [21]. Simplified approaches are indeed recommended for pedestrian structures with $f_v <$ 3 Hz.

For the case-study system, based on Equation (6), the limit acceleration peak a_{max} = 0.7 m/s^2 can be hence taken into account ($f_v = f_{es}$ = 15.1 Hz), and no additional vibrational checks are required. As shown in Figure 10, the EC0-A2 provisions and the experimental estimates for the examined structure result in fact in mostly satisfied serviceability performances, for all the considered test scenarios (i.e., with "acceptable" acceleration peak for 24 configurations, over 26). The exception is represented by the CN#3 and #4 scenarios (in-place jump, p = 1), while few other configurations (four in total) are approaching the vibration acceptability limit. Two of them (CN#1 and #2) are still associated to an impulsive excitation (p = 1), while the CN#8 and CN#11 configurations have a relatively high occupation density (with normal walking activity).

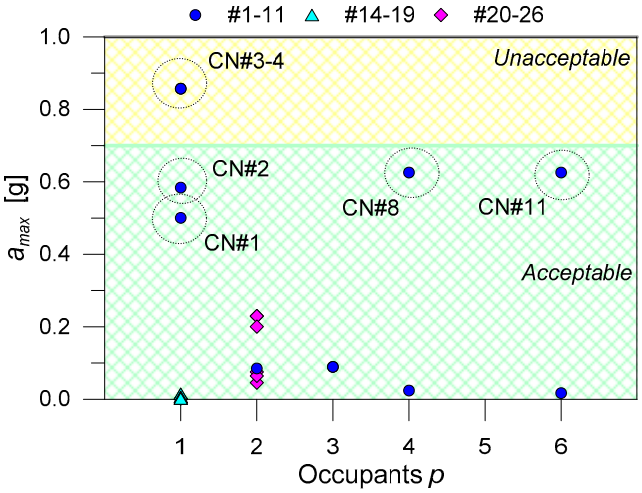

Figure 10. Vibration serviceability assessment of the examined system, based on EC0-A2 provisions. Experimental acceleration peaks (average values, vertical direction), as a function of the number of occupants.

For ordinary floors or special pedestrian structures requiring advanced calculation methods against vibrations, the Eurocode 0 follows the ISO recommendations [22]. There, the limit acceleration peaks (in %g) are provided as a function of the "ISO baseline curve", based on the destination of the structure, the class of use and the key movement features (see Figure 11). The proposed acceleration thresholds are more restrictive especially for the frequency range of 4 Hz to 8 Hz, where unpleasant effects are expected for the human body [51]. Certainly, the ISO method is simple and efficient for design practice. On the other hand, research studies highlighted that the approach (and other criteria in which the vibration thresholds are provided as a function of the structural frequency only) can have intrinsic limits when applied to pedestrian systems with reduced mass ([56,57], etc.), like the walkway herein explored and glass structures in general.

When the ISO criterion is applied to the examined system, see Figure 11, it is possible to notice that most of the CN#n configurations could still satisfy the recommended comfort limits. For few of them only (five in total, with four associated to an in-place jump (p = 1)) the threshold performance for

"indoor footbridges" is exceeded. Three further conditions are approaching the limit peak, while the majority of them suggests a relatively good dynamic behavior of the structure.

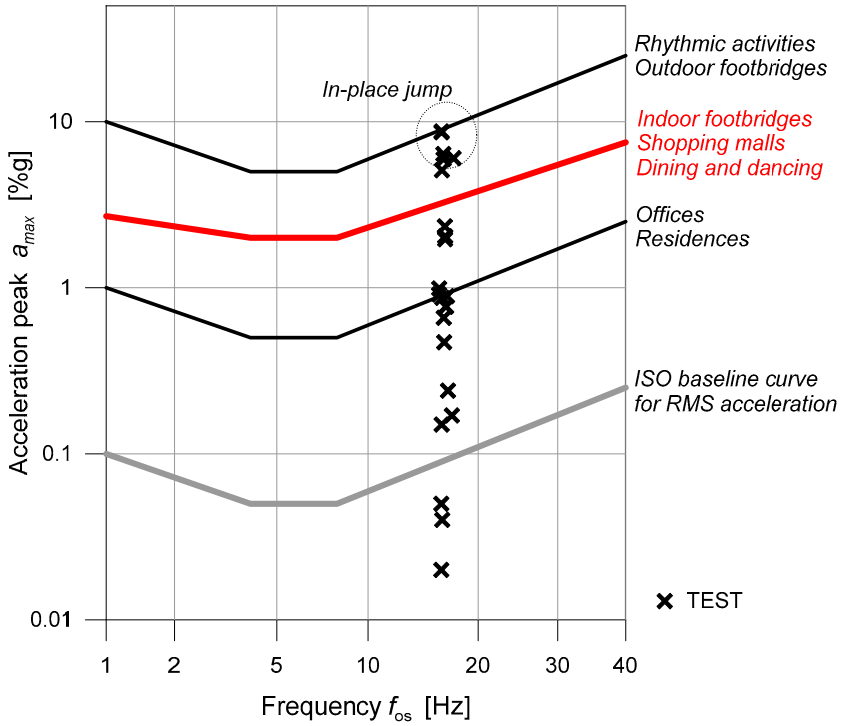

Figure 11. Vibration serviceability assessment of the examined system, based on ISO recommended limits. Experimental acceleration peaks (average values, vertical direction), as a function of the corresponding frequency.

5.3.2. SÉTRA Guideline

In accordance with the SÉTRA document, a first classification of a given pedestrian system should be carried out as a function of the frequency of the structure, see Table 4 and [23]. The desired comfort level must be then satisfied by checking the expected acceleration peak a_{max} in service conditions. Four classes of use can be in fact detected, depending on the occupation density of the system object of analysis:

Class I	Urban footbridges with very heavy traffic
Class II	Urban footbridges with heavy traffic
Class III	Footbridges for standard use
Class IV	Seldom used footbridges

Table 4. Reference frequency and acceleration ranges (vertical direction) for the comfort assessment according to [23].

Frequency Assessment			Acceleration Assessment		
Range	**Frequency (Hz)**	**Resonance Risk**	**Range**	**Acceleration Peak (m/s^2)**	**Comfort Level**
F1	1.7–2.1	Maximum	A1	0–0.5	Maximum
F2	1–1.7 or 2.1–2.6	Medium	A2	0.5–1	Medium
F3	2.6–5	Low	A3	1–2.5	Minimum
F4	0–1 or >5	Negligible	A4	>2.5	Not acceptable

For a mean occupation in the order of d = 0.5 p/m^2 (see Table 2), a "class III" of use can be taken into account for the case-study walkway. Given the experimental frequency of the empty system (f_{es} = 15.1 Hz), however, and according to SÉTRA recommendations, the structure can be classified in a

"frequency range 4" with "negligible risk" of resonance and null discomfort for the occupants. Specific dynamic analyses are in fact required by SÉTRA only for pedestrian systems that fall in the classes I-to-III, or when the vertical frequency is lower than 5 Hz, disregarding the structural typology and the fundamental dynamic features.

The maximum acceleration peak a_{max} due to a single, equivalent occupant should be in fact calculated as:

$$a_{max} = \frac{1}{2\xi} \cdot \frac{4p(t)w_d}{\rho_s \pi} \tag{7}$$

where w_d = 1.65 m is the available width of the deck and ρ_s the total linear density (sum of deck and pedestrian). The harmonic pedestrian load $p(t)$ should be then estimated based on the class of use (III) and frequency range (4) of the examined walkway. Its general definition gives:

$$p(t) = Pcos\left(2\pi f_p t\right)\frac{n'}{S}\psi \tag{8}$$

with P = 280 N the pedestrian force (class III), S the walking surface (1.65 × 2.65 = 4.375 m^2); f_p the walking frequency (with 1.6–2.4 Hz for "normal" activity). In Equation (8), n' is the equivalent number of perfectly synchronized pedestrians (corresponding to a stream of n pedestrians), given by:

$$n' = 10.8\sqrt{\xi n}\left(\text{for } d < 1\text{p/m}^2\right) \tag{9}$$

with ξ the critical damping. Finally, ψ is the reduction coefficient that accounts for the probability that f_p (or its second harmonic) approaches f_{os}. For a vertical frequency f_{os} < 1 Hz or > 2.6 Hz, however, the SÉTRA document suggests ψ = 0, hence $p(t)$ = 0 (Equation (7)) and a_{max} = 0, based on Equation (8).

In Figure 12, comparative results are proposed for the experimental acceleration peaks of the glass walkway, as a function of p and f_{os}. Differing from EC0-A2 and ISO provisions, it can be noticed that the majority of CN#n configurations are associated to "maximum" comfort, while six of them fall in the "medium" level. Again, the configurations with "medium" vibration performance are characterized by an in-place jump (p = 1), see Figure 12b. Few others, however, are related to high occupation density and normal walking conditions (CN#8 and #11).

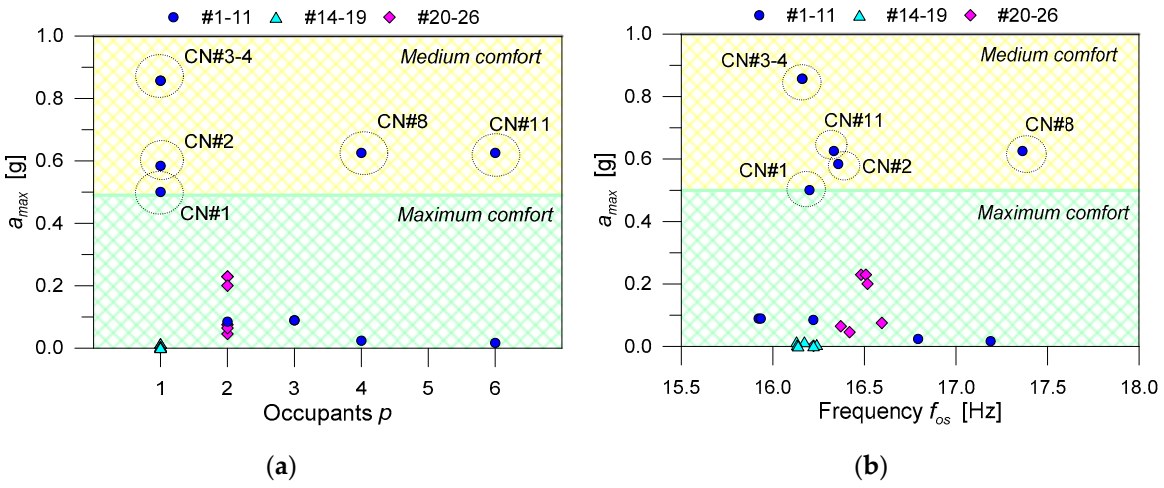

Figure 12. Vibration serviceability assessment of the examined system, based on the SÉTRA guideline document. Experimental acceleration peaks (average values, vertical direction), as a function of (**a**) number of occupants and (**b**) frequency.

5.3.3. AISC Design Guide 11

The North American AISC document was finally taken into account. The document is based on a simplified approach that was specifically calibrated for framed steel floors of 20–30 years ago

(with typical vertical frequency in the range from 5 Hz to 8 Hz). As a result, the method is not able to correctly reproduce the dynamic performance of recent systems (i.e., lightweight concrete, etc.), or structures with frequencies below 5 Hz or above 8 Hz. For pedestrian structures with frequency higher than 9–10 Hz, moreover, the AISC document recommends an additional "stiffness verification", to ensure appropriate performances under concentrated loads [24].

The vibration verification can be conventionally carried out by comparing the expected acceleration ($100 \times a_{max}$/g):

$$100 \cdot \frac{a_{max}}{g} = \frac{P_o exp(-0.35 \cdot f)}{\beta W} \leq 100 \cdot \frac{a_{lim}}{g} \quad (10)$$

with the corresponding limit value, given as a function of the class of use of the system (a_{lim} = 5%g for "outdoor" footbridges; a_{lim} = 1.5%g for "indoor structures" and a_{lim} = 0.5%g for "churches").

In Equation (10), P_0 is a constant force representing the walking excitation (0.41 kN for indoor footbridges and 0.29 kN for churches), f is the fundamental frequency (in Hz), β the modal damping ratio (0.01 for indoor footbridges, 0.02 for churches) and W the effective weight (in kN) sustained by steel beams, joists of girder panes (as applicable).

For the examined walkway, given $f = f_{es}$ = 15.1 Hz and W = M_{glass}, it is possible to notice that the inequality of Equation (10) clearly results in unsatisfactory vibration performances, with a maximum acceleration up to 4.59%g > 1.5%g ("indoor footbridges", that is ≈3.15 the exceedance ratio). Even considering that the pedestrian system is realized in a church, Equation (10) would provide unpleasant acceleration ratios (1.62%g > 0.5%g, ≈3.24 the exceedance ratio), see Figure 13a,b.

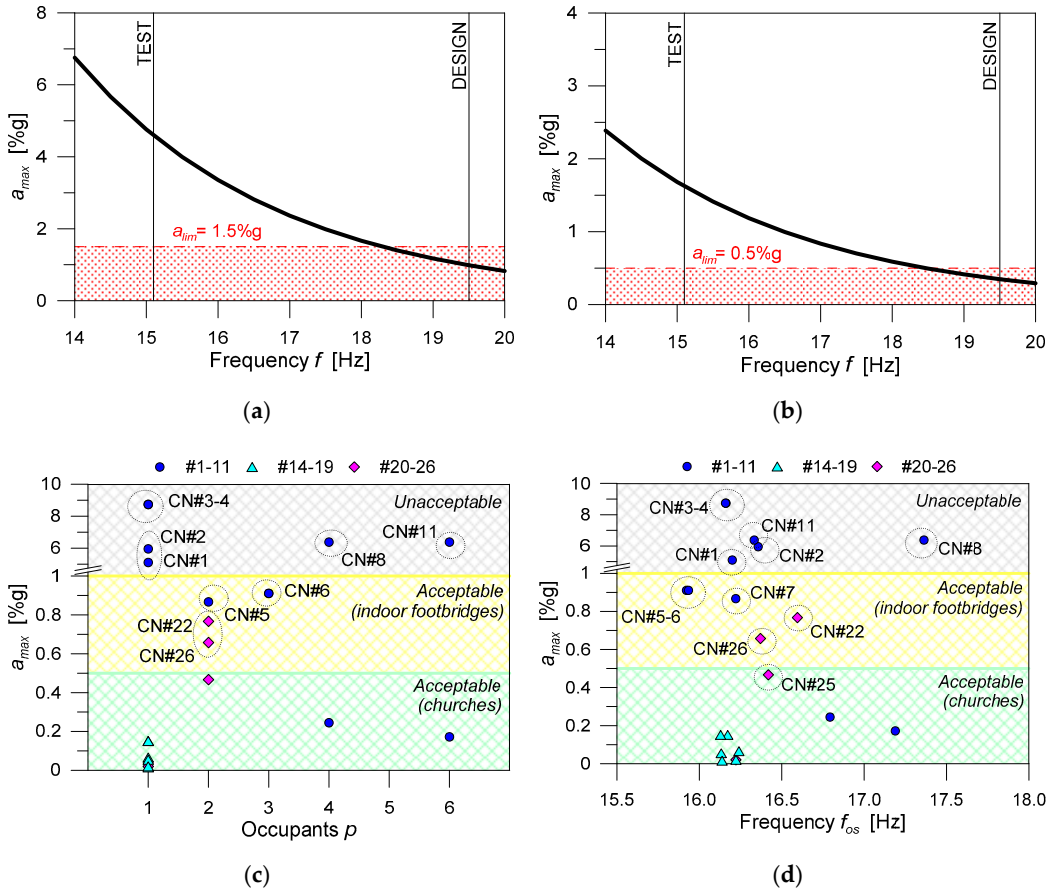

Figure 13. Vibration serviceability assessment of the examined system, based on the AISC technical guide. Expected acceleration peaks, based on Equation (10), for (**a**) indoor footbridges and (**b**) church systems, with (**c**,**d**) assessment of experimental acceleration peaks (average values, vertical direction), as a function of the number of occupants or frequency.

Besides the intrinsic uncertainty that derives from the application of the AISC methodology to a glass pedestrian system with dynamic features that do not match the original criterion, it is interesting to notice in Figure 13a,b that the "design" performance of the glazed structure would be still able to satisfy the vibration serviceability requirements (with 1.06%g < 1.5% for "indoor footbridges" and 0.37%g < 0.5%g for "church" structures). Otherwise, as far as the PVB stiffness decreases, the vertical frequency of the walkway also decreases and results in unfavorable comfort estimates, hence emphasizing the key role of continuous maintenance interventions and monitoring programs for glass structures. In Figure 13c,d, it is also worth mentioning the actual comfort classification of the system, with respect to the AISC recommended limits. The distinction is made in terms of acceleration peaks (%g), as a function of p and f_{os}. As shown, in both the cases, for nine of the tested scenarios (≈1/3rd the experimental campaign) the measured accelerations are "unacceptable" and do not satisfy the "indoor footbridge" threshold value (1.5%g). Up to 14 loading configurations (≈1/2nd the experimental study) are above the acceleration limit for "churches". The imposed threshold condition is hardly satisfied even in presence of a limited number of occupants (i.e., p = 1–2), due to the intrinsic flexibility of the glazed structure.

6. Definition of Perception Index and Perception Scales for Glass Pedestrian Systems

6.1. Acceleration Peaks and Perception Index (PI) Values

The "perception index" (PI) value, as also shown in [37,55,58,59], etc., allows us to quantify the feeling of walking/standing occupants over a given pedestrian structure. It hence represents a parameter of interest for structural assessment considerations, especially for existing footbridges or for new structures including innovative technologies and materials.

In the case of the glass system discussed herein, an intrinsic limit of the PI estimates could be represented by the size of the independent panels (and thus, by the number of occupants that can be involved simultaneously). On the other side, the collected PI values can support the development of dedicated comfort analysis methods, specifically calibrated for glass structures. The human perception of vibrations (even at low amplitudes) can be in fact magnified by psychological effects, hence resulting in possible additional unfavorable feelings. Structural glass in buildings, in this regard, can be sometimes recognized by the occupants as an "unsafe" material [60,61], and such an unpleasant perception is reasonably expected to further increase in presence of transparent walking surfaces (see Figure 3).

During the experimental campaign, the perception of vibrations from the involved volunteers was collected for each test scenario of Table 2. Based on [37], the PI values were calculated as:

$$PI = \frac{1}{N}\sum_{i=1}^{5} W_i \cdot n_i \tag{11}$$

with n_i denoting the number of volunteers choosing the i-th W_i grade and N the total number of involved occupants. Five perception grades were hence detected, i.e., "imperceptible" (W_i = 1), "just perceptible", "obviously perceptible", "unpleasant/annoying" and "intolerable" (W_i = 5).

In Table 5 and Figure 14, the obtained perception estimates are shown. It is important to notice that the number of occupants reflects the actual size of the examined walking surface. Given the class of use of the structure (monumental/religious building), in addition, the CN#n configurations can be considered well representative of the typical operational condition for the examined system.

Table 5. Perception grade records for the test CN#*n* scenarios.

Test Scenario	Occupants		Vibration	Perception Grade				
	Total	Density	a_{max}	Imperceptible	Just Perceptible	Obviously Perceptible	Unpleasant/Annoying	Intolerable
	p	p/m^2	(%g)	($W_i = 1$)	($W_i = 2$)	($W_i = 3$)	($W_i = 4$)	($W_i = 5$)
CN#1	1	0.228	8.74	-	-	-	-	1
CN#2	1	0.228	5.95	-	-	-	1	-
CN#3	1	0.228	8.63	-	-	-	-	1
CN#4	1	0.228	5.10	-	-	-	1	-
CN#5	2	0.457	0.91	-	-	1	1	-
CN#6	3	0.686	0.99	-	-	1	2	-
CN#7	3	0.686	0.87	-	-	1	2	-
CN#8	4	0.914	0.24	-	-	3	1	-
CN#9	4	0.914	6.38	-	-	1	-	3
CN#10	6	1.372	0.17	-	2	3	1	-
CN#11	6	1.372	6.02	-	1	3	2	-
CN#14	1	0.228	0.15	-	-	1	-	-
CN#15	1	0.228	0.11	-	-	1	-	-
CN#16	1	0.228	0.07	-	1	-	-	-
CN#17	1	0.228	0.05	-	1	-	-	-
CN#18	1	0.228	0.02	-	1	-	-	-
CN#19	1	0.228	0.04	-	1	-	-	-
CN#20	2	0.457	2.34	-	-	-	1	1
CN#21	2	0.457	1.96	-	-	-	2	-
CN#22	2	0.457	0.77	-	-	2	-	-
CN#23	2	0.457	2.04	-	-	-	1	1
CN#24	2	0.457	0.47	-	-	2	-	-
CN#25	2	0.457	0.66	-	-	2	-	-
CN#26	2	0.457	0.89	-	-	1	1	-

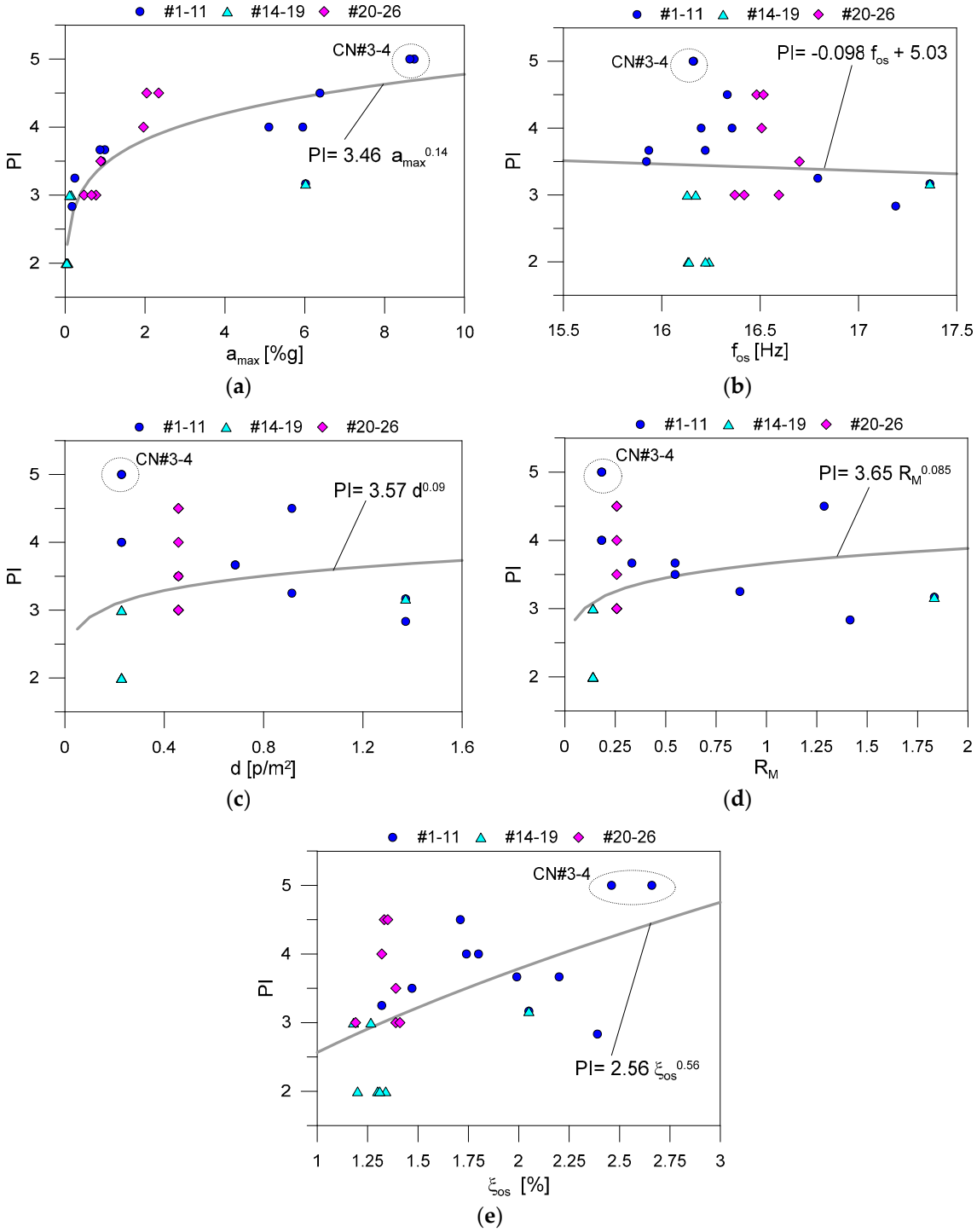

Figure 14. Perception Index (PI) values for the examined system, as a function of (**a**) acceleration peak a_{max}; (**b**) frequency f_{os}; (**c**) occupation density d; (**d**) added mass ratio R_M; (**e**) damping ξ_{os}.

In Figure 14a–d, PI values are reported as a function of the acceleration peak a_{max} (%g), frequency f_{os}, occupation density d, added mass ratio R_M and modal damping ξ_{os}. From the collected data, it is possible to notice that:

- as a_{max} increases, PI also increases, with a mostly exponential trend, which appears slightly affected by p or by the movement features (Figure 14a);
- all the PI values tend to stabilize and start to decrease when the corresponding f_{os} increases, as a direct effect of the added global stiffness of the occupied system (Figure 14b);

- the occupation density d, see Figure 14c, seems a poor parameter for the detection of the PI trend. As shown, the (PI-d) data are mostly scattered and a clear correlation between PI estimates from different walking scenarios can be hardly perceived;
- the added mass ratio R_M, which is partly related to d, could provide a more accurate description of the walking setup and of the overall dynamic response of the examined structure. As shown in Figure 14d, for small R_M values (i.e., 0.15–0.20), the corresponding PI data are still sensitive to the movement features. In contrary, the PI values tend to rapidly stabilize with the increase of R_M;
- the PI values, finally, generally increase with ξ_{os} (see Figure 14e). This effect is implicitly related to the imposed amplitude of vibrations (increasing with PI) and to the effects of added mass from the occupants.

At the same time, however, it is important to remind that:

- a further refinement of the collected perception grades requires a wide set of experimental data (especially for testing scenarios with high walking frequencies);
- generally, in such a kind of comfort evaluations, psychological effects are difficult to define and quantify, and can vary significantly among the involved individuals [55]. Accordingly, a given setup configuration should be tested involving different volunteers;
- in the specific case of pedestrian glass systems, an additional influencing parameter for psychological reactions to the imposed movements can be certainly represented—at least for some of the involved volunteers—by the transparency of the walking surface. The limited size/number of restraints, with respect to the walking surface, can also manifest in a possible discomfort increase (i.e., Figure 3);
- finally, it is reasonably expected that the occurrence of minimum noise during the walking experiments (i.e., due to the vibrating glass members over the steel tendons and the unilateral point restraints, see Figure 6) could represent an additional influencing parameter of interest for the feeling assessment of the volunteers, thus resulting in a potential magnification of human perceptions and annoyance, even at low levels of vibration [60,61].

6.2. Perception Scales for Comfort Assessment

In conclusion, following [37], the PI estimates for the vertical vibrations of the examined glass walkway were associated to a comfort level class that identifies five groups:

-	Very good	VL-1	when	$1 \leq PI \leq 1.5$
-	Good	VL-2		$1.5 < PI \leq 2.5$
-	Normal	VL-3		$2.5 < PI \leq 3.5$
-	Bad	VL-4		$3.5 < PI \leq 4.5$
-	Intolerable	VL-5		$4.5 < PI \leq 5$

It was shown in Figure 14 that—for a large number of the CN#n configurations—the in-service system should be classified with a global "bad" response (with a mean PI = 3.54, corresponding to VL-4). Even excluding the CN#1-to-#4 scenarios (p = 1, in-place jump), the scale perception would be only slightly modified (i.e., "normal" vibration performance (VL-3), with a mean PI = 3.35). As a result, the collected PI estimates would generally suggest the need of retrofit interventions, to ensure an optimal dynamic performance of the structure. The same subjective feelings, however, can provide further relevant feedback, as far as the collected data are compared with comfort levels and quantitative walking features.

In Figure 15a, a possible analytical correlation of PI grades is hence proposed for the case-study system, as a function of the reference VL classes and walking frequencies f_p. There, the average f_p is derived—for each CN#n configuration—from the corresponding experimental records. The mean walking frequency for "normal" activity is also emphasized in the figure (dashed lines). The second-order fitting curve of the experimental PI data shows that under "normal" activities the structure can be still associated to "normal" or even "good" performances. The comfort level decreases,

in contrary, as far as "unconventional" walking frequencies are imposed to the system. For some CN#*n* conditions, it is worth mentioning that a "weak" comfort level was perceived by the volunteers, even in the presence of "normal" walking activities, but random movement and high occupation density (VL-4 range in Figure 15a). Such an outcome reflects the class of use of the system, where it is rationally expected to have high occupation density and a combination of several movement features (especially frequencies) that do not match with "normal" parameters (i.e., when the visitors move by small groups, standing on the system, etc.).

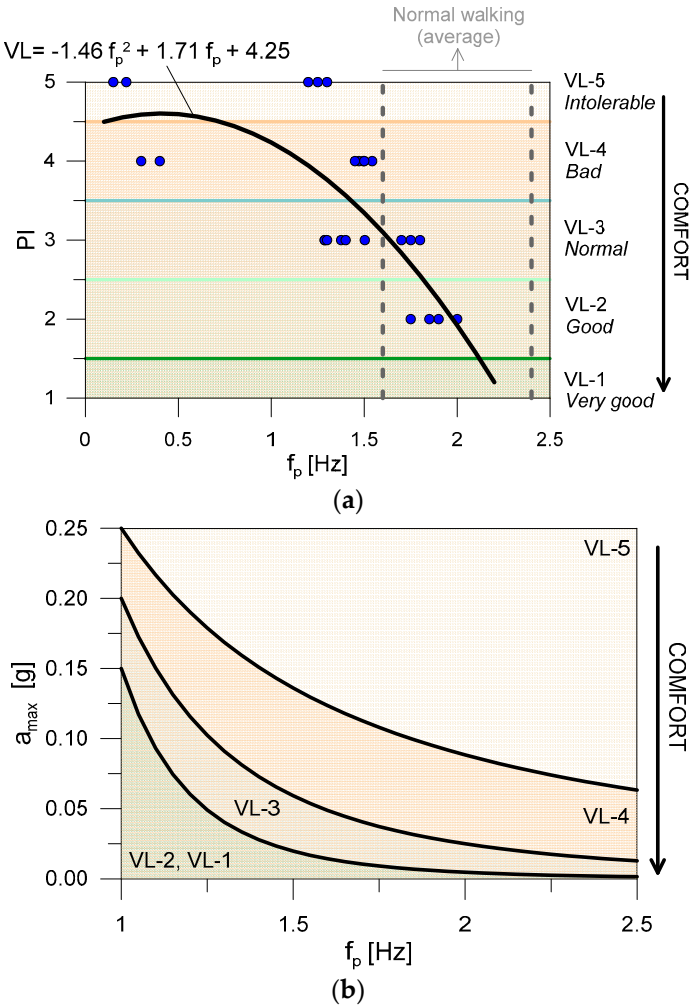

Figure 15. Analytical correlation between (**a**) experimental walking frequencies f_p and corresponding vibration comfort levels VL (vertical direction) for the examined system, and (**b**) definition of possible perception curves for graphical comfort assessment.

The advantage of Figure 15a is hence that the comfort performance of the in-service structure can be assessed for a given walking frequency f_p, accounting also for the specific structural typology and destination. Otherwise, it does not consider other relevant movement features, like the imposed acceleration peak. It was in fact shown in [37] that PI-a_{max}-f_p plots derived from experiments can offer a suitable tool for comfort estimates. A similar approach is hence proposed in Figure 15b, where fitting curves are obtained from the experimental data, including movement features (walking frequency, acceleration peak) and perception feelings from the volunteers. As shown, as far as a "normal" walking activity is taken into account, it is possible to notice that "good" or "normal" perception feelings of the volunteers are associated to relatively low acceleration peaks, up to a maximum of 0.07–0.08 g. When the walking frequency decreases and/or the acceleration peak increases, the perceived comfort rapidly

reduces. Such an outcome is mostly associated to relatively low acceleration amplitudes, compared to the threshold values in use by standards for "maximum vibration comfort" (see Section 5.3).

In conclusion, it can be hence stated that:

- the collected experimental records and feedback generally suggested the need of analysis and verification methods that are specifically calibrated for glass systems, with intrinsic geometrical and mechanical features that do not match with other structural typologies or traditional materials in use for footbridges;
- at the same time, in accordance with several literature studies, the experimental outcomes of Figure 15 confirmed that the vibration serviceability assessment of pedestrian structures is a complex design issue, involving multiple aspects. The added value of the current study is to point out that key influencing parameters for glass systems must be explored both on the structural/dynamic side (i.e., system features, sensitivity to human induced loads, etc.) and especially on the psychological side (i.e., subjective human reactions). For the examined walkway, the sensitivity of volunteers' feelings to the transparency of the pedestrian surface was emphasized. Another relevant parameter—even at low vibration amplitudes—could be represented by possible noise of glass components and metal supports, hence resulting in added annoyance for the occupants. In this regard, further dedicated studies involving a large number of volunteers would allow to further validate and generalize the actual observations.

7. Conclusions

In this paper, the vibration performance of an in-service glass walkway was investigated based on field experiments, existing analytical methods and perception scales. The dynamic behavior and sensitivity of pedestrian systems to human-structure interaction (HSI) phenomena is a key research topic, especially with respect to flexible/innovative structural typologies or to the effects of unfavorable operational conditions/possible damage in a given structure. This is also the case of pedestrian glass structures, where a combination of intrinsic geometrical/mechanical features requires dedicated studies, both at the design stage but also during the service life. For the walkway herein discussed, a wide set of experimental configurations was taken into account (26 in total, involving 20 adults, various movement features and two ambient conditions), in order to explore its dynamic response and assess the actual vibration comfort levels.

In terms of dynamic features of the occupied system, it was shown that frequency variations up to +15–20% could be generally expected, in comparison to the empty walkway. The damping capacity of the system was also found to increase, in the order of two times the empty structure, when changing the number of occupants and the movement features.

In terms of comfort level assessment, several analytical methods available in the literature for pedestrian structures were taken into account, namely the Eurocode 0—Annex A2 provisions, the SÉTRA guideline document and the AISC Design Guide. It was shown that while these documents (and others) offer simplified graphical and/or single-degree-of-freedom (SDOF) approaches to estimate the maximum expected vibration effects and verify the required comfort criteria of a given pedestrian structure, most of them are specifically calibrated for limited walking scenarios/structural typologies. Their reliability to real case-studies (especially light structures) needs consequently continuous validation. As far as the key parameter is the maximum acceleration peak due to human movements, in particular, the vibration comfort level for the explored glass walkway was found to be relatively "good" according to the Eurocode recommendations, "medium"/"maximum" based on the SÉTRA guideline, but also "unacceptable" for several testing conditions, according to the AISC document.

In this regard, the definition of "perception index" values can offer further feedback for comfort evaluations (and the definition of possible retrofit interventions). The advantage is that the vibrational check can be carried out based on a combination of experimental measurements (i.e., acceleration peaks and occupied frequencies), subjective feelings from the occupants (i.e., perception grades) and movement features (i.e., walking frequency, etc.). For the case-study glass system, it was shown that

the in-service structure would still offer a "good" vibrational performance under ordinary walking activity (with 1.6–2.4 Hz the mean movement frequency). On the other hand, for walking frequencies that do not match the reference range for "normal" movement (and this is in line with the destination of the structure, where visitors are expected to move by small groups, standing/walking slowly on the glazed system), the corresponding comfort was found to partly decrease, even to "bad" levels. More detailed vibration serviceability can be hence carried out by relating the walking features (frequency and acceleration peak, in this study) and the comfort feelings of the occupants, that in the case of transparent pedestrian surfaces could be further magnified by relevant psychological effects (even in presence of relatively low vibration amplitudes). The final result, as shown, can take the form of design charts that are specifically calibrated to account for the intrinsic features of in-service glass structures.

Author Contributions: This paper results from a joint collaboration of both the authors.

Funding: This research received no external funding. The APC was funded by MDPI (review vouchers of the first author).

Acknowledgments: The "Società per la conservazione della Basilica"—So.Co.Ba. Foundation is gratefully acknowledged for facilitating the experimental measurements.

Conflicts of Interest: The authors declare no conflict of interest.

References

1. Haldimann, M.; Luible, A.; Overend, M. *Structural Use of Glass*; IABSE: Zurich, Switzerland, 2008; ISBN 978-3-85748-119-2.
2. Feldmann, M.; Kasper, R.; Abeln, B.; Cruz, P.; Belis, J.; Beyer, J.; Colvin, J.; Ensslen, F.; Eliasova, M.; Galuppi, L.; et al. Guidance for European structural design of glass components—Support to the implementation, harmonization and further development of the Eurocodes. In *Report EUR 26439–Joint Research Centre-Institute for the Protection and Security of the Citizen*; Dimova, S., Pinto, A., Feldmann, M., Denton, S., Eds.; Office of the European Union: Luxembourg, 2014. [CrossRef]
3. CNR-DT 210/2013. Istruzioni per la Progettazione. In *L'esecuzione ed il Controllo di Costruzioni con Elementi Strutturali in Vetro*; National Research Council (CNR): Roma, Italy, 2013.
4. Biolzi, L.; Bonati, A.; Cattaneo, S. Laminated glass cantilevered plates under static and impact loading. In *Advances in Civil Engineering*; Yepes, V., Ed.; Hindawi Publishing Corporation: London, UK, 2018; Volume 2018, p. 7874618. [CrossRef]
5. Bedon, C.; Kalamar, R.; Eliasova, M. Low velocity impact performance investigation on square hollow glass columns via full-scale experiments and Finite Element analyses. *Compos. Struct.* **2017**, *182*, 311–325. [CrossRef]
6. Veer, F.A.; Bristogianni, T.; Baardolf, G. A case study of apparently spontaneous fracture. *Glass Struct. Eng.* **2018**, *3*, 109–117. [CrossRef]
7. Corradi, M.; Speranzini, E. Post-cracking capacity of glass beams reinforced with steel fibers. *Materials* **2019**, *12*, 231. [CrossRef]
8. Zhang, X.; Bedon, C. Vulnerability and protection of glass windows and facades under blast: Experiments, methods and current trends. *Int. J. Struct. Glass Adv. Mater. Res.* **2017**, *1*, 10–23. [CrossRef]
9. Dotan, H. Zhangjiajie grand canyon glass bridge. In Proceedings of the Challenging Glass 5—Conference on Architectural and Structural Applications of Glass, Gent, Belgium, 16–17 June 2016; ISBN 978-90-825-2680-6.
10. Krstic-Furundzic, A.; Kosic, T.; Terzovic, J. Architectural aspect of structural glass roof design. In *COST Action TU0905 Mid-Term Conference on Structural Glass*; Belis, J., Louter, C., Mocibob, D., Eds.; CRC Press: Boca Raton, FL, USA, 2013; ISBN 978-1-138-00044-5.
11. Cai, J.; Xu, Y.; Feng, J.; Zhang, J. Design and analysis of a glass roof structure. In *The Structural Design of Tall and Special Buildings*; Xilin, L., Ed.; John Wiley & Sons Ltd.: Hoboken, NJ, USA, 2013; Volume 22, pp. 677–686. [CrossRef]
12. Lauriks, L.; de Bow, M.; Wouters, I. Glass in Roofs. Study of the 19th Century Literature on Building Technology. In Proceedings of the 1st WTA International PhD Symposium, Leuven, Belgium, 8–9 October 2009.

13. Bijster, J.; Noteboom, C.; Eekhout, M. Glass entrance Van Gogh Museum Amsterdam. *Glass Struct. Eng.* **2016**, *1*, 205–231. [CrossRef]
14. Davis, B.; Avci, O. Simplified vibration serviceability evaluation of slender monumental stairs. *J. Struct. Eng.* **2015**, *141*. [CrossRef]
15. Andreozzi, L.; Briccoli Bati, S.; Fagone, M.; Ranocchiai, G.; Zulli, F. Weathering action on thermo-viscoelastic properties of polymer interlayers for laminated glass. *Constr. Build. Mater.* **2015**, *98*, 757–766. [CrossRef]
16. Bedon, C.; Fasan, M.; Amadio, C. Vibration analysis and dynamic characterisation of structural glass elements with different restraints based on Operational Modal Analysis. *Buildings* **2019**, *9*, 13. [CrossRef]
17. Clough, R.W.; Penzien, J. *Dynamics of Structures*; McGraw-Hill: New York, NY, USA, 1993; ISBN 0-07-011394-7.
18. Shahabpoor, E.; Pavic, A.; Racic, V. Interaction between walking humans and structures in vertical direction: A literature review. *Shock Vib.* **2016**, *2016*, 3430285. [CrossRef]
19. ABAQUS. *ABAQUS Computer Software V. 6.14*; Dassault Systémes: Providence, RI, USA, 2017.
20. Bedon, C. Diagnostic analysis and dynamic identification of a glass suspension footbridge via on-site vibration experiments and FE numerical modelling. *Compos. Struct.* **2019**, *216*, 366–378. [CrossRef]
21. EN 1990. *Eurocode 0—Basis of Structural Design—Annex A2: Application for Bridges*; CEN: Brussels, Belgium, 2005.
22. ISO 10137. *Bases for Design of Structures—Serviceability of Buildings and Walkways Against Vibrations*; International Organization for Standardization (ISO): Geneva, Switzerland, 2007.
23. SÉTRA. Assessment of vibrational behavior of footbridges under pedestrian loading. In *SÉTRA Technical Guide*; Technical Department for Transport, Roads and Bridges Engineering and Road Safety: Paris, France, 2006.
24. Murray, T.M.; Allen, D.E.; Ungar, E.E.; Davis, D.B. Floor vibration due to human activities. In *Steel Design Guide Series*, 2nd ed.; Griffis, G.L., Ed.; American Institute of Steel Construction (AISC): Chicago, IL, USA, 2016; Volume 11.
25. Koutsawa, Y.; Daya, E.M. Static and free vibration analysis of laminated glass beam on viscoelastic supports. *Int. J. Solids Struct.* **2007**, *44*, 8735–8750. [CrossRef]
26. Pelayo, F.; Lopez-Aenlle, M. Natural frequencies and damping ratios of multi-layered laminated glass beams using a dynamic effective thickness. *J. Sandw. Struct. Mater.* **2017**, *21*. [CrossRef]
27. Zemanova, A.; Zeman, J.; Janda, T.; Schmidt, J.; Sejnoha, M. On modal analysis of laminated glass: Usability of simplified methods and enhanced effective thickness. *Compos. Part B Eng.* **2018**, *151*, 92–105. [CrossRef]
28. Ramos, A.; Pelayo, F.; Lamela, M.J.; Fernandez Canteli, A.; Huerta, C.; Pacios, A. Evaluation of damping properties of structural glass panes under impact loading. In *COST Action TU0905 Mid-Term Conference on Structural Glass*; Belis, J., Louter, C., Mocibob, D., Eds.; CRC Press: Boca Raton, FL, USA, 2013; ISBN 978-1-138-00044-5.
29. Bedon, C.; Amadio, C. Numerical assessment of vibration control systems for multi-hazard design and mitigation of glass curtain walls. *J. Build. Eng.* **2018**, *15*, 1–13. [CrossRef]
30. Feng, Q.; Fan, L.; Huo, L.; Song, G. Vibration reduction of an existing glass window through a viscoelastic material-based retrofit. *Appl. Sci.* **2018**, *8*, 1061. [CrossRef]
31. Bachmann, H.; Ammann, W. *Vibrations in Structures Induced by Man and Machines*; Structural Engineering Documents, International Association of Bridge and Structural Engineering (IABSE): Zurich, Switzerland, 1987; Volume 3e.
32. Muhammad, Z.; Reynolds, P.; Avci, O.; Hussein, M. Review of pedestrian load models for vibration serviceability assessment of floor structures. *Vibration* **2019**, *2*, 1–24. [CrossRef]
33. Busca, G.; Cappellini, A.; Manzoni, S.; Tarabini, M.; Vanali, M. Quantification of changes in modal parameters due to the presence of passive people on a slender structure. *J. Sound Vib.* **2014**, *333*, 5641–5652. [CrossRef]
34. Setareh, M.; Gan, S. Vibration testing, analysis and human-structure interaction studies of a slender footbridge. *J. Perform. Constr. Facil.* **2018**, *32*, 040018068. [CrossRef]
35. Feldmann, M.; Heinemeyer, C.; Butz, C.; Caetano, E.; Cunha, A.; Galanti, F.; Goldack, A.; Hechler, O.; Hicks, S.; Keil, A.; et al. *Design of Floor Structures for Human Induced Vibrations*; EUR 24084 EN; European Commission Joint Research Centre: Aechen, Germany, 2009; ISBN 978-92-79-14094-5. [CrossRef]
36. Heinemeyer, C.; Butz, C.; Keil, A.; Schlaich, M.; Goldack, A.; Trometer, S.; Lukic, M.; Chabrolin, B.; Lemaire, A.; Martin, P.O.; et al. *Design of Lightweight Footbridges for Human Induced Vibrations*; EUR 23984 EN; European Commission Joint Research Centre: Aechen, Germany, 2009; ISBN 978-92-79-13387-9. [CrossRef]

37. Ma, R.; Ke, L.; Wang, D.; Chen, A.; Pan, Z. Experimental study on pedestrian's perception of human-induced vibrations of footbridges. *Int. J. Struct. Stabil. Dyn.* **2018**, *18*, 1850116. [CrossRef]
38. Toso, M.A.; Gomes, H.M.; Silva, F.T.; Pimentel, R.L. Experimentally fitted biodynamic models for pedestrian-structure interaction in walking situations. *Mech. Syst. Sig. Process.* **2016**, *72–73*, 590–606. [CrossRef]
39. Whittington, B.R.; Thelen, D.G. A simple mass-spring model with roller feet can induce the ground reactions observed in human walking. *J. Biomech. Eng.* **2009**, *131*, 011013. [CrossRef]
40. Matsumoto, Y.; Griffin, M.J. Dynamic response of the standing human body exposed to vertical vibration: Influence of posture and vibration magnitude. *J. Sound Vib.* **1998**, *212*, 85–107. [CrossRef]
41. Jones, C.A.; Pavic, A.; Reynolds, P.; Harrison, R.E. Verification of equivalent mass-spring-damper models for crowd-structure vibration response prediction. *Can. J. Civ. Eng.* **2011**, *38*, 1122–1135. [CrossRef]
42. Silva, F.T.; Brito, H.M.B.F.; Pimentel, R.L. Modeling of crowd load in vertical direction using biodynamic model for pedestrians crossing footbridges. *Can. J. Civil Eng.* **2013**, *40*, 1196–1204. [CrossRef]
43. Cao, L.; Qi, H.; Li, J. Experimental and numerical studies on the vibration serviceability of fanshaped prestressed concrete floor. *Int. J. Distrib. Sens. Netw.* **2018**, *14*. [CrossRef]
44. Abeysinghe, C.M.; Thambiratnam, D.P.; Perera, J.N. Dynamic performance characteristics of an innovative hybrid composite floor plate system under human-induced loads. *Compos. Struct.* **2013**, *96*, 590–600. [CrossRef]
45. Soltis, L.A.; Wang, X.; Ross, R.J.; Hunt, M.O. Vibration testing of timber floor systems. *For. Prod. J.* **2002**, *52*, 75–81.
46. Da Silva, J.G.S.; Vellasco, P.C.G.S.; de Andrade, S.A.L. Vibration analysis of orthotropic composite floors for human rhythmic activities. *J. Braz. Soc. Mech. Sci. Eng.* **2008**, *1*, 56–65. [CrossRef]
47. Bedon, C.; Bergamo, E.; Izzi, M.; Noè, M.S. Prototyping and validation of MEMS accelerometers for structural health monitoring—The case study of the Pietratagliata cable-stayed bridge. *J. Sens. Actuator Netw.* **2018**, *7*, 30. [CrossRef]
48. SMIT. Structural Modal Identification Toolsuite. Available online: http://smit.atlss.lehigh.edu (accessed on December 2018).
49. Chang, M.; Leonard, R.L.; Pakzad, S.N. SMIT User's Guide. Release 1.0. Available online: http://smit.atlss.lehigh.edu/wp-content/uploads/2012/07/SMIT-Users-Guide.pdf (accessed on 2018).
50. Chang, M.; Pakzad, S.N. Observer kalman filter identification for output-only systems using interactive structural modal identification toolsuite. *J. Bridge Eng.* **2014**, *19*, 04014002. [CrossRef]
51. Gheitasi, A.; Ozbulut, O.E.; Usmani, S.; Alipour, M.; Harris, D.K. Experimental and analytical vibration serviceability assessment of an in-service footbridge. *Case Stud. Nondestruct. Test. Eval.* **2016**, *6*, 79–88. [CrossRef]
52. Van Nimmen, K.; Lombaert, G.; Roeck, G.D.; Broek, P.V.D. Vibration serviceability of footbridges: Evaluation of the current codes of practice. *Eng, Struct.* **2014**, *59*, 448–461. [CrossRef]
53. Dey, P.; Walbridge, S.; Narasimhan, S. Vibration serviceability analysis of aluminum pedestrian bridges subjected to crowd loading. In Proceedings of the 6th International Conference on Advances in Experimental Structural Engineering, University of Illinois, Urbana, IL, USA, 1–2 August 2015.
54. Smith, A.L.; Hicks, S.J.; Devine, P.J. *Design of floors for vibration: A new approach*; The Steel Constriction Institute (SCI): London, UK, 2009; p. 354. ISBN 1-85942-176-8.
55. Leonard, D. *Human Tolerance Levels for Bridge Vibrations*; TRRL Report No. 34; Road Research Laboratory: Wokingham, UK, 1966.
56. Knudsen, J.S.; Grathwol, N.; Hansen, S.O. Vibrational response of structures exposed to human-induced loads. In *36th IMAC—A Conference and Exposition on Structural Dynamics 2018*; Gaetan, K., Ed.; Springer: Berlin, Germany, 2018; pp. 151–158.
57. De Silva, C.W. *Vibration and Shock Handbook*; CRC Press: Boca Raton, FL, USA, 2005; ISBN 978-1-4200-3989-4.
58. Chen, P.W.; Robertson, L.E. Human perception thresholds of horizontal motion. *J. Struct. Div.* **1972**, *98*, 1681–1695.
59. Ebrahimpour, A.; Sack, R.L. A review of vibration serviceability criteria for floor structures. *Comput. Struct.* **2005**, *83*, 2488–2494. [CrossRef]

60. Pavelchak, M.A. Evaluation of vibration problems in existing office buildings. In Proceedings of the EVACES2017—Experimental Vibration Analysis for Civil Engineering Structures, San Diego, CA, USA, 12–17 July 2017; pp. 736–745. [CrossRef]
61. Cerpinska, M.; Irbe, M. Specifics of natural frequency measurements for floor vibration. *Eng. Rural Dev.* **2017**, 162–166. [CrossRef]